ADVANCED FUNCTIONAL MATERIALS
www.afm-journal.de

Materials Fabrication from Native and Recombinant Thermoplastic Squid Proteins

*Abdon Pena-Francesch, Sergio Florez, Huihun Jung, Aswathy Sebastian, Istvan Albert, Wayne Curtis, and Melik C. Demirel**

Natural elastomers made from protein extracts have received significant interest as eco-friendly functional materials due to their unique mechanical and optical properties emanating from secondary structures. The next generation sequencing approach is used to identify protein sequences in a squid ring teeth complex extracted from *Loligo vulgaris* and the use of recombinant expression is demonstrated in the fabrication of a new generation of thermoplastic materials. Native and recombinant thermoplastic squid proteins exhibit reversible solid to melt phase transition, enabling them to be thermally shaped into 3D geometries such as fibers, colloids, and thin films. Direct extraction or recombinant expression of protein based thermoplastics opens up new avenues for materials fabrication and synthesis, which will eventually be competitive with the high-end synthetic oil based plastics.

1. Introduction

Thermoplastics comprise a unique class of polymers that become moldable above a specific temperature. Thermoplastics synthesized from natural building blocks include proteins and polysaccharides. Because of their advantages including well-defined structural features, unique shapes and sizes, genetic programmability (only for proteins), and robust chemistries, these macromolecules offer substantial opportunities for functional materials fabrication.[1] However, industrial costs and sustainable resources are major competitive disadvantages for natural materials. Therefore, heterologous expression of natural materials provides an alternative source for economically feasible and sustainable protein-based thermoplastic production.[2]

Functional eco-friendly, protein-based materials include various elastomeric proteins (e.g., silk[3]), soy protein[4]), protein gels (e.g., biomaterials scaffolds[5]) and modular elastomer-like proteins (e.g., poly-peptides[6]). They provide similar or enhanced mechanical, optical, and biological properties relative to synthetic alternatives.[7] Retaining these properties in recombinantly expressed proteins remains a challenge.[2] Using next generation sequencing (NGS)[8] in conjunction with high throughput proteomics,[9] Guerrette et al.[10] recently introduced an approach to rapidly identify genes that encode for a specific proteinaceous material candidate. This sets the stage for heterologous expression, purification and materials processing. The NGS approach thereby provides access to the genetic resource of a wide range of biological elastomeric materials that occur in species whose genomes have not yet been sequenced. Biomimicry of the material properties identified in the NGS and/or expression phases would ultimately enable large scale, low cost production of these properties.

Squid ring teeth (SRT) is a thermoplastic protein complex[11] extracted from the suction cups of squid tentacles. Compared to other bio-derived thermoplastics[7] (e.g., keratin, resilin, elastin), the proteinaceous structure of the SRT[11] does not have any covalent cross-linkers and hence, dissolves in polar protic or weak alkaline/acidic buffers.[12] Further, SRT reversibly agglomerates if the solvent is removed.[13]

In a recent collaborative effort, Guerrette et al.[10] studied recombinant expression of a protein from a SRT complex, and demonstrated processing to complex shapes by solution based methods. Although the native SRT complex is thermoplastic, the recombinant SRT protein did not replicate these thermoplastic properties. In the current work, we studied a smaller protein from the SRT complex, and show that its recombinant expression successfully produces a thermoplastic protein. We identified the protein sequences in a SRT complex extracted

A. Pena-Francesch, H. Jung, Prof. M. C. Demirel
Materials Research Institute and Department of Engineering Science and Mechanics
Pennsylvania State University
University Park
PA 16802, USA
E-mail: mdemirel@engr.psu.edu
S. Florez, Prof. W. Curtis
Department of Chemical Engineering
Pennsylvania State University
University Park
PA 16802, USA
A. Sebastian, Dr. I. Albert
Bioinformatics Consulting Center
Pennsylvania State University
University Park
PA 16802, USA
A. Sebastian, Dr. I. Albert, Prof. M. C. Demirel
Huck Institutes of Life Sciences
Pennsylvania State University
University Park
PA 16802, USA

DOI: 10.1002/adfm.201401940

from *Loligo vulgaris* using the NGS approach, and demonstrate recombinant expression for its use in the fabrication of a new generation of thermoplastic materials. This new material exhibits reversible solid to melt phase transition, enabling it to be thermally shaped into 3D geometries such as fibers, colloids, and thin films. In addition to its unique capability to be thermally remodeled into multiple functional forms such as colloids, fibers, thin films and nanotextured surfaces, we also showed that both native and recombinant SRT has excellent mechanical properties in wet and dry conditions that exceed most natural thermoplastics.

2. Results and Discussions

Squid is an invertebrate cephalopod in the phylum Mollusca[12] that lives in cold sea water (i.e., 5–15 °C) and uses its limbs and suckers for a variety of tasks including holding prey, locomotion, and behavioral displays.[14] It has evolved teeth inside its suction cups, which serve to secure its grasp on underwater prey. European common squid (*Loligo vulgaris*) used for this study were caught off the coast of Tarragona, Catalonia (**Figure 1**a). The SRT was removed from the tentacle suctions cups as shown (Figure 1b). The morphology of the tissue surrounding SRT was imaged by electron microscopy (Figure 1c). Fluorescence microscopy of the epithelium tissue with green (nucleus dye) and red (f-actin) staining shows the columnar shape of these cells (Figure 1d). The Maldi-TOF and SDS PAGE of the SRT protein complex show proteins of varying sizes between 18 kDa to 52 kDa (Figure S1, Supporting Information).

An extensive characterization of the SRT protein was carried out to explore its polymeric properties for producing thermoplastic materials. The mechanical properties of the SRT protein complex were studied by multiple thermal characterization techniques. Isolated SRT was processed to form a highly viscous melt. Importantly, the term "melt," as used herein, does not refer to a phase transition, (i.e., from solid to liquid[15], but instead refers to a glass transition. The thermal characteristic of the protein film was studied using Differential Scanning Calorimetry (DSC). The glass transition temperature, T_g, in water was observed as the inflection in heat flow at 32 °C (**Figure 2**a). When heated above 196 °C, the protein complex degraded as indicated by the downward spike in heat-flow observed in the DSC data (Figure 2b). The high temperature exothermic degradation[16] was most likely due to destabilization of the protein structure[17] and oxidation of the amino acids at this elevated temperature (i.e., an apparent color change of the film from white to yellow).

The viscoelastic characteristics of the protein film were studied using Dynamical Mechanical Analysis (DMA). The SRT protein complex was molded into thin ribbons to perform stress-strain analysis under dry or wet conditions. These viscoelastic measurements were performed at 20 °C (below T_g) so that the SRT would generally behave as a solid as shown in Figure 2c. In contrast, when the tensile experiment was performed in water (i.e., a plasticizer) at 55 °C (above T_g), the SRT deformed like

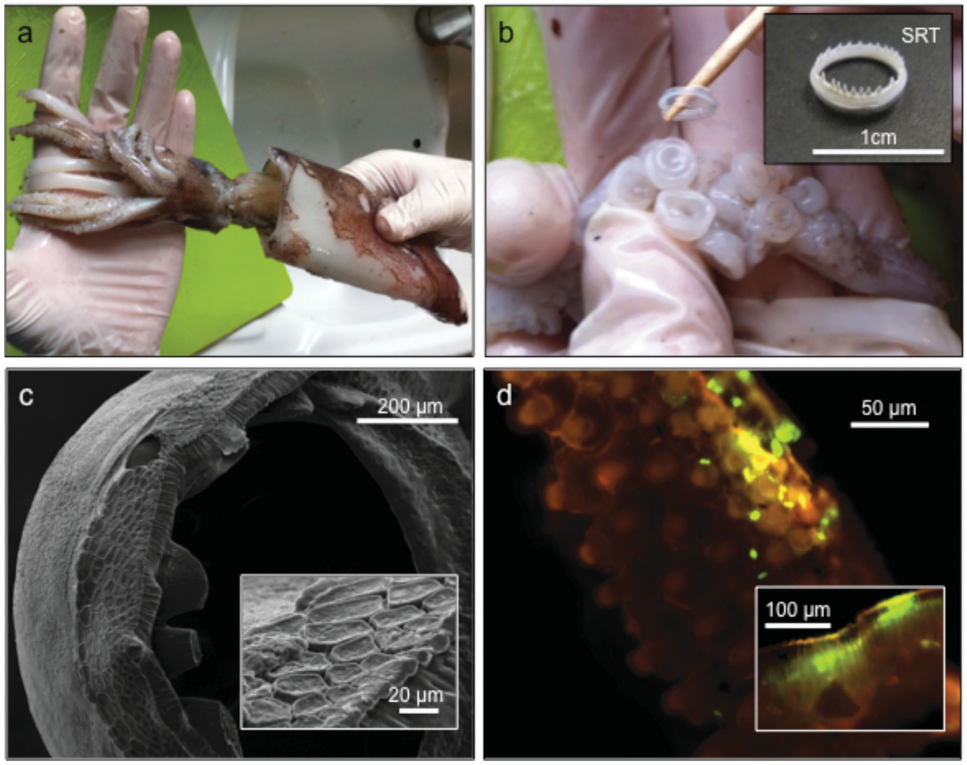

Figure 1. Squid ring teeth (SRT) collection and characterization: a) European common squid (*Loligo vulgaris*) is caught in the Mediterranean Sea near Taragona. b) SRT is removed from the suction cups along the arms and tentacles using a toothpick. c) Electron microscopy of the suction cups reveals a columnar epithelium (inset). d) Suction cup tissue is characterized by targeting F-actin with phalloidin dyes and nuclei with DAPI staining with a fluorescence microscopy. Inset shows the fluorescence image of the tissue cross section.

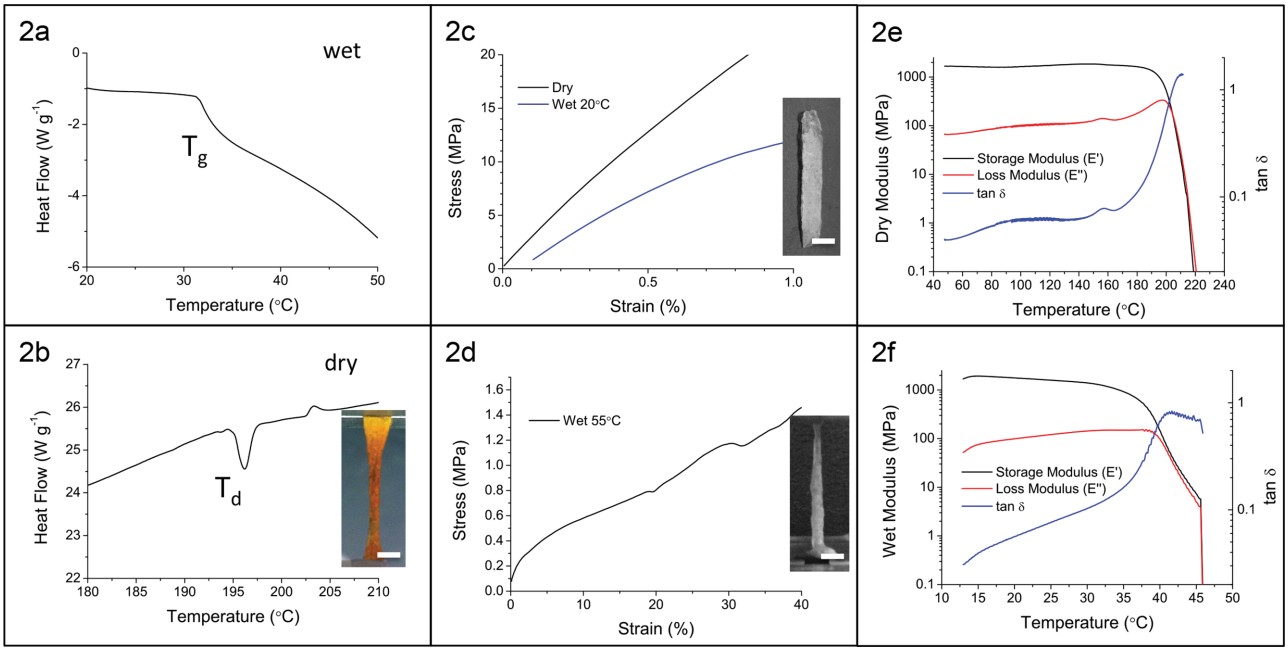

Figure 2. DSC heat flow of SRT powder in water shows a) glass transition at 32 °C (T_g) and b) denaturation at 196 °C (T_d). Color change (inset b) indicates oxidation of the protein film. Stress-strain curves for c) dry or wet SRT films at 20 °C and d) wet film at 55 °C ($T > T_g$) are shown. The ribbon sample (inset in (c)) deforms viscoelastically (inset in (d)) above T_g. e) Oscillatory DMA temperature sweep in dry conditions shows a stable mechanical behavior below 196 °C and a sharp drop at 210 °C above degradation temperature, T_d. T_g for dry case is between 160–180 °C. Scale bar is 2 mm for all optical images. f) Oscillatory DMA temperature sweep in wet conditions reveals a transition around 35 °C, where the protein begins to flow and the modulus decreases.

a viscoelastic melt. Similar to elastin,[18] the modulus of the protein melt above T_g was approximately 10 MPa (Figure 2d). The DMA test showed similar values for the dynamic elastic modulus in dry (1.9 ± 0.1 GPa) and underwater (1.1 ± 0.1 GPa) conditions at room temperature. The original stiffness value was retained in both conditions after multiple "melt recycling" of the protein (Figure S6, Supporting Information). A similar range of elastic modulus has been reported for the native Humboldt SRT via nanoindentation[19] (i.e., 2.5–3.5 and 5.0–7.0 GPa for wet and dry, respectively) at room temperature; however, the previous work had not presented the complete thermal response presented here. The dry storage modulus (Figure 2e), displayed a stable modulus over a large range of temperatures (25 to 196 °C), which dropped sharply above the denaturing temperature T_d = 196 °C. The wet storage modulus (i.e., elastic component) slowly decreased with increasing temperature until it reached the glass transition temperature (Figure 2f). At this temperature, the film deformed viscoelastically with respect to the tension, and the modulus dropped significantly.

The novel modular structure of the SRT permitted deformation into nearly any geometry with a diverse array of processing methods. As a viscoelastic melt, processing of SRT was very similar to thermoplastics. Therefore, conventional processing approaches can be applied to this material such as injection molding, extrusion, and annealing. Preparation of the protein melt was an easy and reversible process where the protein powder was shaped into different geometries via extrusion molding in hot water (above its T_g). The recyclability of the protein melt can be exploited by molding it repeatedly into any 3D geometry, from simple curved ribbons (**Figure 3**a) to colloids (Figure 3b) as well as lithographic patterns (Figure 3c) and nanotubes (Figure 3d). Colloids of SRT were created both by thermal annealing from solid phase as well as by surfactant induced aggregation from solution phase. Figure 3b demonstrates the effect of surface tension on the smoothing of a colloid from an irregular SRT powder. Furthermore, the thermal recyclability of the protein can be exploited by molding it into nanoscale objects, such as nanotube arrays (Figure S2a, Supporting Information). The pore diameter can be controlled by the selection of an adequate template membrane with specific pore diameter, length, and distribution. Polycarbonate track-etched membranes (PCTE) with varying pore diameters (i.e., 0.4 µm, 0.8 µm and 5 µm as shown in Figure 3d and Supporting Information Figure S2b,c respectively) were used as membrane template in this approach. The protein melts into the pores of the membrane via a nanowetting process[20] above its glass transition temperature. The PCTE membranes were chemically etched and the nanotubes were revealed as a continuous nanotube array.

Complex geometry in nanoscale objects can be manufactured by solution casting techniques exploiting the reversible agglomeration of SRT proteins. The protein was dissolved in 5% acetic acid in aqueous solution, then spin-casted to form a thin film on a silicon substrate (Figure 3e). Another fabrication method is nanoparticle synthesis by dissolving the protein in acetic acid, and aggregating using a surfactant (i.e., Sodium dodecyl sulfate). Figure S3a shows that particle size is controllable with this approach and an average particle diameter of 100 nm particles was obtained. These particles were characterized by the dynamic light scattering (DLS). The protein particles were

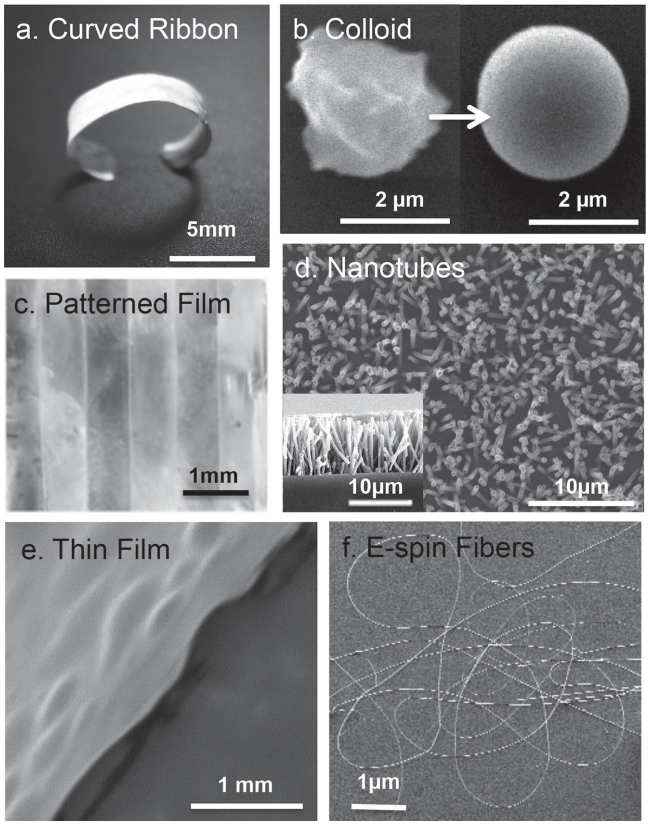

Figure 3. Extrusion molding and solution processing of the native SRT: a) curved ribbons, b) colloids, c) lithographic patterned film, and d) 400 nm diameter nanotubes were formed through extrusion of the protein powder. Solution casting and electrospinning was employed for e) thin film and f) microfibers manufacturing respectively.

easily dissolved in weakly acidic solutions (Figure S3b, Supporting Information).

Different methods of fiber extrusion include melt (i.e., simplest and least expensive technique), wet (i.e., fibers that require solvent dissolution), dry (i.e., fibers with a melt temperature close to their thermal degradation temperature), dry-jet wet (i.e., high performance fibers with a liquid crystal structure), and electro-spinning.[21] In this study, SRT fibers were obtained via electro-spinning (Figure 3f). Formation of these fibers was tested through three methodologies to optimize the elongation of the fiber and to control its diameter. First, we dissolved SRT in 5% acetic acid aqueous solution. SRT is positively charged[13] in this solvent and dissolves homogenously. Ethanol was added to the solution in equal parts to increase the yield of electrospinning. However, the fiber density was low (Figure S4a, Supporting Information). Moreover, SRT fibers or films dissolve slowly due to a trace of acedic acid, which binds strongly to proteins depending on the pH. Second, SRT was dissolved in hexafluoro-2-propanol (HFIP), which is a good polar solvent for proteins (e.g., commonly used in amyloid research). Figure S4b (Supporting Information) shows the formation of fibers through SRT-HFIP solution, which improved the fiber density as well as increased the fiber length. The average fiber diameter is 0.5 μm. Although, uniform fiber formation was observed in HFIP, this solvent has a high vapor pressure, and it is corrosive. Therefore, we switched to poly-ethylene-oxide (PEO), which is commonly used as a biomaterial due to its biocompatibility, hydrophilicity, and versatility. Figure S4c (Supporting Information) shows the fiber generated using SRT-PEO mixture, which had a diameter of 2 μm. The PEO has leached out from the fiber (Figure S4d, Supporting Information). This method also provides formation of fibers of uniform diameter without end beads.

A combination of RNA-sequencing and protein mass spectroscopy was performed to identify several proteins of the SRT complex. mRNA extracted from the suction cups of the epithelium tissues of *Loligo vulgaris* was sequenced to identify the cDNA that aligned with the protein sequences observed in the SRT complex. A schematic of the overall process of identifying SRT proteins is shown in **Figure 4**. High throughput sequencing produced 10 160 143 paired-end reads, with a read length of at least 250 base pairs, which was used to assemble a preliminary transcriptome (Figure 4a). Peptide sequences from the whole SRT protein complex were sequenced using mass-spectrometry, to provide N-terminal biased partial protein sequences that were matched against the putative transcripts (Figure 4b). Details of the iterative bioinformatics approach can be found in supplementary information, and outlined briefly below. The primary transcriptome assembly was initiated using Trinity software.[8] This process produced roughly 30 000 putative transcripts that represent mRNA from cells that form the suction cups. By comparison, in the model small genome pigmy squid, just over 1100 putative protein coding sequences were recently identified.[22] The distinct protein structure of the SRT provides a means to dramatically narrow the focus to a limited subset of nucleotide sequences. The peptide sequences produced via the mass-spectrometry allowed us to identify the Trinity assembled preliminary transcripts that most closely matched the SRT protein fragments of interest. A final narrowing of the focus was based on the presence of extensive beta-sheet structures (e.g., AVSHT-rich) known to be present in the SRT and the general ability to identify the beta-sheet structure from the primary protein sequence. The transcripts that matched all three sources of bioinformatic analysis were considered "candidate fragments" for the SRT proteins of interest.

The next stage of SRT gene discovery involved combining the candidate fragments to identify whole genes. Utilizing the entire dataset of sequencing reads, the candidates were extended in both directions with an aligner that utilized read end overlap. The extension concatenation process was repeated until the start and stop codons were identified to create a complete putative coding sequence for the full transcripts. The final stage, to confirm the predicted full-length transcripts, utilized 5′ and 3′ RACE (Rapid Amplification of cDNA Ends) using Clonetech's SMARTER cDNA synthesis kit (Figure 4c and Supporting Information Figure S5). The sequenced 5′ RACE results confirmed the predicted start codon, and the 3′RACE was used to confirm the remainder of the sequence. We note that the transcriptome assembly may fail because of an internal repeating region in the genomic sequence, which is common in bioelastomers. For example, RACE PCR results for the largest SRT protein revealed 105 extra amino acids after amino acid 343 that was omitted in the predicted sequences of 52 kDa SRT proteins. Within this 105 amino acid sequence, there was a

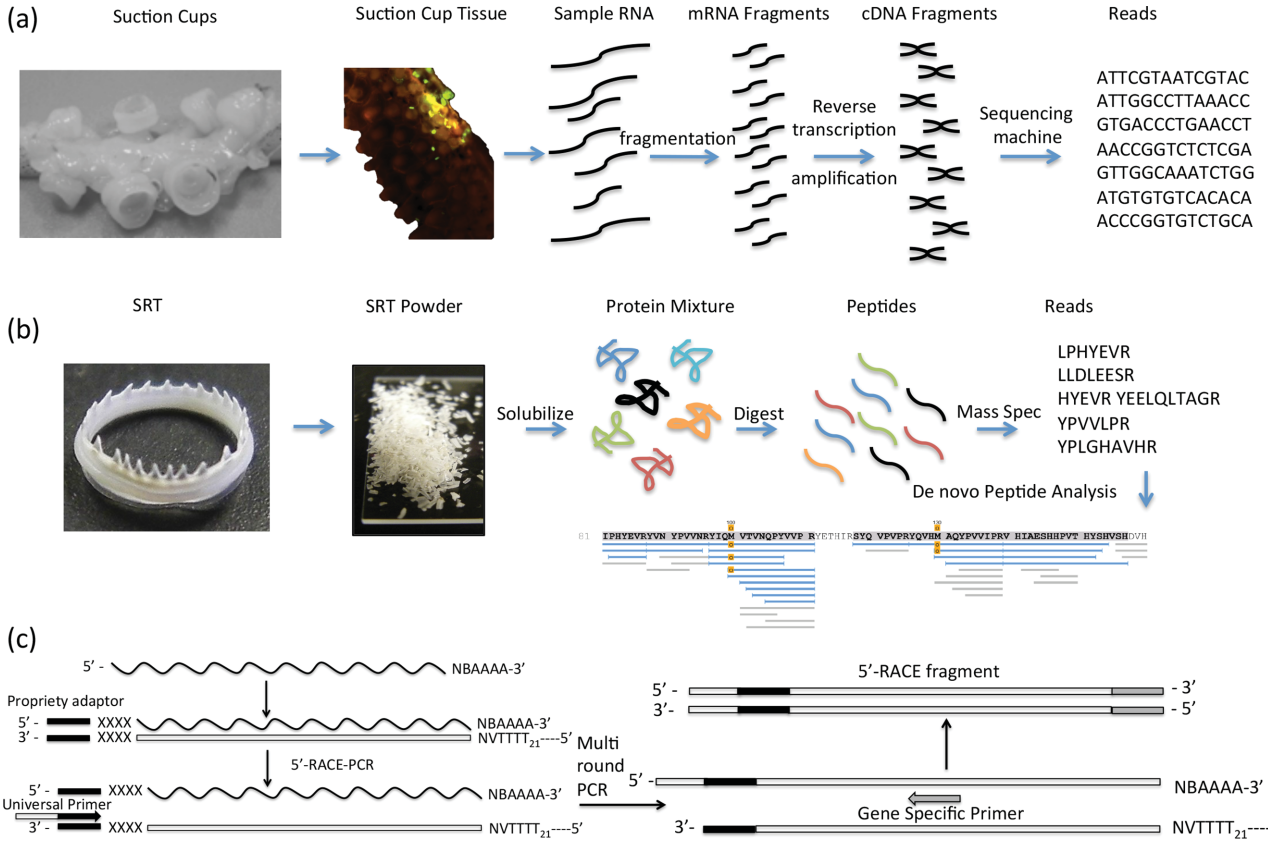

Figure 4. Next generation sequencing using squid suction cups and SRT protein. a) transcriptome assembly, b) proteomics, c) race PCR for gene sequence validation. See text for details.

70 amino acid region having an 80% identity with a downstream sequence. Additional annotation of the SRT protein is provided below with the bioinformatics identification (**Figure 5**). The SignalP software[23] predicted the signal peptide to be the first 20 amino acids of the protein sequence (Figure S5, Supporting Information).

Direct extraction of SRT from squid tentacles is limited due to price and natural sources (e.g., ≈0.1 g of SRT could be extracted per kg of squid). Therefore, recombinant expression of SRT proteins could provide sustainable thermoplastic production. In our previous collaborative work, Guerrette et al.[10] demonstrated expression of a 39 kDa protein of SRT extract from *Dosidicus gigas* (almost the double the size of LvSRT-18 kDa), but this protein lacked the melt phase transition, and hence materials fabrication was only demonstrated in the solution phase. Similarly, LvSRT-54 kDa protein lacks the melt phase transition in wet conditions. Polymer chain's local concentration scales inversely with the square root of polymer size ($\sim N^{-1/2}$), as first suggested by Flory,[24] and hence a smaller protein would most likely demonstrate the desired melt phase due to increased number of hydrogen bonding.[25] Hence, recombinant expression of the smallest known SRT protein (≈18 kDa) extracted from *Loligo vulgaris* (LvSRT) was performed. This is based on the isolated intact genes, generated by high-fidelity PCR of the cDNA, created from the tissue surrounding the SRT and presumed to contribute substantially for assembly of the ring teeth structure. To obtain the recombinant LvSRT, the full length sequence was cloned into Novagen's pET14b vector system and transformed into *E. coli* strain BL21(DE3). Recombinant SRT expression was obtained with a purity of ≈90% and an estimated yield of ≈50 mg/L. The yield increases approximately ten times (i.e., ≈0.5 g/L) in the auto induction media.[26] The size of the protein was confirmed via an SDS-page gel (**Figure 6**a).

Materials fabrication, including solvent and thermal based methods, is demonstrated using purified recombinant SRT. Based on our earlier experience with native SRT, a concentration of 1 to 100 mg/mL of recombinant SRT can be achieved in the HFIP solvent. Figure 6b shows circular film casted from LvSRT dissolved in HFIP. However, casting has limitations when it comes to fast and continuous industrial production of plastic films. Thermoplastic processes, used in the plastic industry are considered preferable because drying steps are eliminated, thereby accelerating their processing times. Water is added to the protein as a plasticizer to improve processability and to modify the properties of the final structure. The thermal characteristics of the recombinant protein were studied using the DSC. The glass transition temperature, T_g, in water is observed as the inflection in heat flow at 34 °C (Figure 6c). Utilization of extrusion and injection-molding technologies has the advantage of offering low cost and versatile production systems. Figure 6d–f shows thermoplastic molding, fiber extrusion, nanotube thermoforming respectively in recombinant LvSRT manufacturing.

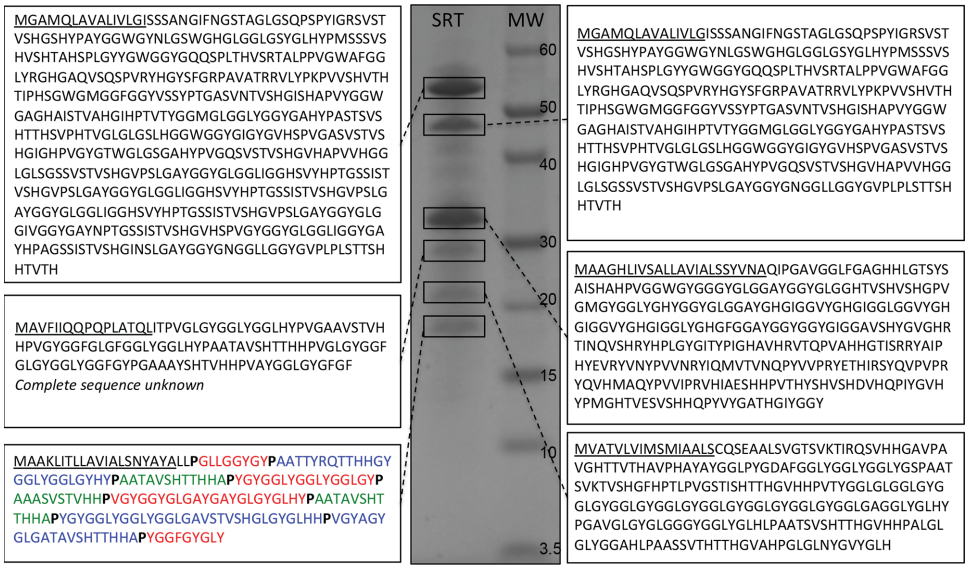

Figure 5. Six protein sequences of SRT complex are identified using an NGS approach and transcriptome assembly. These sequences show varying sizes between 18 kDa to 52 kDa as demonstrated by the SDS-Page (middle). 48 kDa and 58 kDa proteins are isoforms. The first 20 amino acids are the signal peptide, which is underlined. Although the NGS approach is a powerful technique for sequence determination, one of the proteins (28 kDa) in the SRT complex could only be partially identified (second sequence on the left). 18 kDa protein is selected for recombinant expression. Tri-block copolymer architecture of the protein sequence is marked as red (Gly-rich), green (AVSHT-rich) and blue (Gly-rich + AVSHT-rich) regions, which are separated by proline residues (bold).

Figure 6. Thermoplastic and solvent based recombinant LvSRT manufacturing is shown. 18 kDa protein is shown in SDS-Page, which is slightly larger (1.5 kDa) due to histidine tag. b) Circular film was fabricated using solvent based casting. c) DSC data shows a glass transition at 34 °C (derivative of the heat flow is shown in the inset) for wet condition. d) Patterned film, e) fiber, and f) nanotubes were manufactured using thermoplastic approach for the first time. g) Load-deflection curves for dry and wet recombinant films at 20 °C ($T < T_g$) are shown. h) Oscillatory DMA temperature sweep of recombinant protein and its comparison to native SRT complex in dry conditions are shown. T_g for dry case is between 160–180 °C.

The mechanical properties of the recombinant protein film were studied using DMA and compression strength test. The recombinant melt sample is brittle and hence compression, instead of tension, tests were performed. The compression dry modulus is approximately twice the wet modulus at room temperature (Figure 6g). The recombinant protein was casted into thin ribbons using HFIP to perform DMA analysis under dry or wet conditions. The dry storage modulus (Figure 6h), displayed a stable modulus (≈1 GPa) over a large range of temperatures (25 to 160 °C), which dropped smoothly at elevated temperatures. The wet modulus showed a smaller value (≈100 MPa) compared to the dry modulus in DMA analysis, which is attributed to solvent (i.e., HFIP) casting of the test sample in water since the modulus drop is also observed for the native SRT (Figure S7, Supporting Information).

3. Conclusion

In summary, versatile materials fabrication techniques were demonstrated for the recombinant LvSRT protein as well as the native SRT protein complex extracted from European common squid to synthesize colloids, thin films, fibers, and nanotube arrays. These materials have remarkable physical properties, which include: i) an elastic modulus of approximately 1 GPa both in aqueous and dry conditions (although the recombinant protein is brittle compared to native SRT), ii) a thermoplastic protein (glass transition of 32 °C for native SRT and 34 °C for recombinant LvSRT-18 kDa in water) that is stable up to 196 °C, and iii) a reversible agglomeration mechanism (e.g., solubility in protic solvents that can break hydrogen bonds or in weakly alkaline/acidic solutions by charge induced dissolution). Understanding the structural and functional characteristics of these novel properties will expedite the design, fabrication and synthesis of eco-friendly, recyclable, advanced materials with functional (i.e., wetting,[27,28] friction[29] and transport[27] characteristics). Recombinant SRT will find use in multiple fields including biomaterials coatings, drug delivery, and membrane filtration. For example, the stimuli responsive switch of SRT based membranes or colloids at weakly acidic or basic conditions could open up new applications in fuel cells and controlled release technologies. Synthesis of SRT-like peptides could also be utilized to manipulate and optimize the materials properties of next generation biomaterials coatings.

4. Experimental Section

SRT Collection: European common squids (*Loligo vulgaris*) were caught from the coast of Tarragona (Spain). The squid ring teeth (SRT) were removed from the tentacles and immediately soaked in deionized water and ethanol mixture (70:30 ratio v/v). After vacuum drying in a desiccator, the rings were pulverized in liquid nitrogen using a ceramic mortar and pestle. Suction cups were stored in RNALater solution (Life Technologies, CA) immediately after capture, and stored in –80 °C refrigerator for subsequent RNA Isolation Protocol and fluorescence microscopy.

RNA Isolation Protocol: Suction cups were defrosted and RNALater solution was decanted. Any remaining SRT in the suction cups was removed to reduce protein contamination. The tissues samples were homogenized by slicing them into smaller pieces with a clean razor inside a biological hood and resuspended in RNAlater solution. The homogenized tissue was disrupted by adding 600 µL of RLT Plus lysis buffer (Qiagen), and kept in room temperature for 2 min (or until the solution color turned yellow) in eppendorf tubes. The solution was centrifuged for 3 min at high speed. For the DNA elimination, the lysate supernatant from last step was transferred to a DNA Eliminator spin column (Qiagen, RNAeasy Mini Kit), and centrifuged for 30 s at 10 000 rpm. 600 µL of 70% ethanol solution was added to the flow through and mixed well by pipetting without centrifugation. For RNA filtering, the solution was transferred to a RNAeasy spin column (Qiagen, RNAeasy Mini Kit) and centrifuged for 15 s at 1000 rpm. Three wash buffer steps were performed according to the Mini Kit user manual. Finally, RNA extraction was completed by adding 50 µL of RNase-free water directly to the spin column membrane, and by collecting the solution via centrifugation for 1 minute at 10 000 rpm. The solution was stored in the fridge for sequencing.

Protein Gel Preparation: 0.2 mg of SRT is dissolved in 1 mL of 5% acetic acid/2 M urea solution, and subjected to sodium dodecyl sulfate polyacrylamide gel electrophoresis (SDS-PAGE) for protein separation. The protein gels were stained with Coomassie blue dye.

Maldi-TOF: 0.25 mg/mL SRT protein solution was prepared in dilute HCl solution at pH = 3. Sample preparation, data analysis, and processing were performed according to the following details. Protein samples were mixed 1:1 with a saturated solution of sinapinic acid in 50% aqueous acetonitrile containing 0.1% trifluoroacetic acid, 1 microliter of this solution was applied to a stainless steel target plate and the samples were allowed to crystallize under ambient conditions. Positive-ion mass spectra were acquired on a Bruker Ultraflextreme MALDI-TOF-TOF instrument operating in linear mode at Penn State Proteomic Center. A factory default method was modified to acquire data over 8000–60 000 m/z range and 15 000 – 70 000 m/z range. Mass spectra were calibrated externally using linear calibration curve and 4 calibrants (Sigma): insulin, cytochrome C ($[M^+H]^+$ and $[M^+2H]2^+$), ubiquitin, and myoglobin ($[M^+H]^+$ and $[2M^+H]^+$). Spectra were smoothed once using Savitzky-Golay algorithm, the baseline subtraction algorithm was TopHat, and the mass lists were generated based on the centroid peak detection algorithm.

Nanotube Array Fabrication: SRT powder (10 mg) was melted in distilled water on a polycarbonate track-etched (PCTE) membrane (Sterlitech, Inc.), using a household microwave (2.45 GHz) oven for 1 min. PCTE membranes with different pore diameters (400 nm, 800 nm and 5 µm) were used. After the deposition, PCTE membranes were immersed in dichloromethane (DCM) at 60 °C for 20 min, which dissolves the template and results in an open nanotube structure connected by a continuous backing of a protein film. The film is kept in ethanol and dried using critical point drying (CPD) to minimize bundling or collapse of the nanotubes.

Scanning Electron Microscopy (SEM): The surface morphology was characterized by an electron microscope (Philips XL30) at an accelerating voltage of 5 kV. Samples were gold coated with a sputter coater (Ladd Research Industries, Model 30800) at 1.6 kV for 75 seconds.

SRT Melting and Thermal Molding: 25 mg of SRT powder was mixed with 10 mL of deionized water at 70 °C ($>T_g$). The powder can be melted at temperatures lower than 70 °C, but it may take a longer time (i.e., >1 minute) to complete the thermal process. The protein was gently pressed to form a flat thin film with an area of 1 cm^2, and then cooled at room temperature. The thickness of the film was approximately 200 µm. The powder may disperse during the melting process due to electrostatic, surface tension and capillary forces. If the film is not uniform, the thermal process could be repeated multiple times. Similarly, the SRT can be thermally molded on to any patterned surface above its glass transition temperature.

SRT Colloids: Two methods for particle fabrication were thermoplastic processing and solution phase synthesis. 2 mg SRT powder was sonicated for 15 min at 60% of output power (Brandson Sonifier 250) to obtain varying sizes of particles. The dispersion was centrifuged at 2000 rpm for 5 min and 50 µL of supernatant was spin coated onto a glass slide (1 cm × 1 cm). Dried samples were immersed in 10 mL of

distilled water at 80 °C for 15 min for thermal processing. The surface tension smoothens irregular SRT particles into a colloid above T_g. For the solution phase synthesis, 1 mg of SRT was dissolved in 1 mL of 5% acetic acid solution (v/v). While stirring, 20 µL of 25 mM sodium dodecyl sulfate (SDS) was added to the solution. To precipitate SRT, the solution was sonicated in an ultrasound bath for 10 minutes and then centrifuged at 6000 rpm for 10 min. The supernatant liquid phase was discarded, and the resulting pellet was resuspended in 1 mL of distilled water and sonicated for 10 min in the ultrasound bath. 50 µL were pipetted on a glass slide, and the remaining water was evaporated overnight at room temperature. The colloids were imaged using electron microscopy.

Differential Scanning Calorimetry: The glass transition temperature, T_g, of the SRT protein complex was determined by a differential scanning calorimeter (Perkin Elmer DSC 8500). 10 mg of SRT with distilled water (1:1 ratio w/w) were mixed and sealed in a 40 µL stainless steel pan. The temperature scanning range was 10 to 90 °C at a heating rate of 5 °C/min.

Fluorescence Microscopy: The suctions cups were washed with distilled water and prepared for cell staining. Actin was labeled using CF 350 conjugated phalloidin (dilution 1:1000) dye for 30 min. Nucleus was stained with 4′-6-diamidino-2-phenylindole (DAPI) dye (1:5000) for 5 minutes. The stained tissue was mounted on a glass slide and imaged with a Leica DM5500B microscope using a 20× objective.

Casting of SRT Thin Films: Two different solvents (acetic acid and hexafluoro-2-propanol, HFIP) were used for casting films. First, 4 mg/mL SRT solution was prepared in 5% of acetic acid (v/v) solution (pH ≈ 3). Second, 20 mg of SRT powder was dissolved in HFIP by sonication for one hour. Both solutions were casted in different molds using 100 µL of the protein solution. Solvent was evaporated at room temperature in the chemical hood, which resulted in a homogeneous protein thin film. The film was peeled from the cast for further characterization.

Electrospinning of Fibers: A vertical electrospinning (e-spin) unit with a copper target was used to produce SRT fibers. Three different solvents (acetic acid in water, HFIP, and PEO mixed with acetic acid in water) were prepared. 10 mg/mL SRT solution in hexafluoro-2-propanol, HFIP (Sigma Aldrich) was prepared by sonication for one hour. Additionally, a mixture of 50 mg of SRT, 5% of polyethylene oxide (PEO, MW 900,000, Sigma Aldrich), and 5% acetic acid were prepared in 5 mL of aqueous solution. The protein solution was loaded into a 5 mL glass syringe for delivery through a 25G syringe needle. The solution was pumped at a rate of 6 mL/h. The voltage was 10 kV between the tip and the collector at a distance of 18 cm. The collected fibers were air dried at room temperature, and they were deposited on a glass substrate for further characterization.

Dynamic Light Scattering (DLS): 2 mg/mL aqueous protein solutions were prepared using acetic acid (5–20% v/v), and the protein size was determined using a Viscotek 802 DLS equipment. The data was analyzed by OmniSIZE software. A 14 µL quartz cell was used for sample analysis. For each spectrum, 10 scans are co-added. Samples were stabilized at 25 °C for 5 minutes before measurement.

LC-MS/MS: 5 mL of chymotrypsin-digested peptides were prepared from SRT aqueous solution. 2 microliters of these peptides were loaded onto an Acclaim PepMap100 trapping column (100 micro-m × 2 cm, C18, 5 micro-m, 100 Å, Thermo) at a flow rate of 20 micro-L/min using 4% aqueous acetonitrile (ACN) as a mobile phase. The peptides were separated on an Acclaim PepMap RSLC column (75 micro-m × 15 cm, C18, 2 micro-m, 100 Å, Thermo) with a 30-min 4–50% linear gradient of acetonitrile in water containing 0.1% formic acid. The gradient was delivered by a Dionex Ultimate 3000 nano-LC system (Thermofisher Scientific) at 300 nL/min. LTQ Orbitrap Velos mass spectrometer (Thermo) was set to acquire data using the following data-dependent parameters: full FT MS scan at R 60,000 followed by 10 ion-trap MS2 scans on most intense precursors with CID activation. Only the precursors with charge states +2 and higher were selected for MS2; monoisotopic precursor selection was enabled, and the isolation window was 2 m/z. PEAKS Studio 5.3 was used for de novo sequence analysis.

Bioinformatics Analyses: This included the quality check of the datasets followed by transriptome assembly. The read trimming quality control tool Trimmomatic was used for the quality check. Adaptor sequences and polyAs were removed from reads. A sliding window trimming was performed, cutting once the average quality within a window size of 4 base pairs falls below 25. Very short reads of <36 base pairs were removed. The clean data set from the quality control step was assembled using Trinity transcriptome assembler with strand-specific RNA sequencing library specification. 33180 transcripts were assembled for *Loligo vulgaris* dataset.

Dataset: European common squid (*Loligo vulgaris*) dataset has been analyzed, and it contained 10 160 143 paired-end reads of 250 bp. Quality control was done using Trimmomatic. Adaptor sequences and polyAs were removed from reads. A sliding window trimming was performed, cutting once the average quality within a window size of 4 base pairs falls below 25. Very short reads of <36 base pairs were removed.

Transcript Assembly: The clean data set was assembled using Trinity with strand specific RNA sequencing library specification using 33180 transcripts.

Blast Search and Short Read Mapping: Peptide sequences from the protein of interest were sequenced using mass-spectrometry (LC-MS/MS). From this, peptides with a confidence score of >50 were searched against trinity-assembled transcripts using tblastn. The blast hits that had alignments with >90% of the length of the peptide and with > = 80% sequence identity were identified as the best hits. These best-hit transcripts were again searched for beta sheets (e.g, ASHVT-rich) using tblastn. The identified transcripts that have both peptide and beta-sheet sequence match were chosen as candidate transcripts. However, since these were not full-length transcripts, further steps were done to identify the full-length candidate transcripts. In order to identify the full-length transcripts, the clean data set was aligned to each of the candidate transcripts using bwa-mem algorithm.[30] Bwa-mem is a short read mapping algorithm. The resulting alignment file was parsed to identify the longest read that mapped to the end of the transcript and was further used to extend the transcript. The entire sets of reads were again mapped to the extended candidate transcript. This process of alignment and extension was repeated until a stop codon is encountered and the transcript is considered to be full-length.

Validation: Identified candidate transcripts were aligned using Clustalw. Further validation was done by checking the amino acid composition. Amino acid composition of all the assembled transcripts were calculated and compared to that of the published data. The candidate transcripts had a composition similar to that of the published dataset.

5′ and 3′ RACE: To confirm the coding sequence of the SRT proteins, a 3′ and 5′ Race was carried out using Clonetech's SMARTer Race cDNA Amplification kit (Clontech Laboratories, Mountain View, CA). The RT-PCR was carried out as specified by the Amplification kit manual using 1 µg of total RNA for both the 3′ and 5′ Race. The resulting cDNA library from the 3′ Race was used to amplify the open reading frame of the Euro gene using a gene specific 5′ primer (5′-ATGGGAGCCATGCAACTAGCGGTG-3′) that was specific for the predicted 5′ UTR. The 3′ primer was the universal primer mix (UPM) that was provided in the kit SMARTer RACE kit. The 5′ Race library was used to confirm the 5′ UTR using the gene specific 3′ primer (5′-TTAGTAGAGACCGTATCCGAAACCTCCA-3′), while the 5′ primer was the UPM. The PCR products were cloned into the PCR4.1 TOPO vector using the TOPO TA cloning kit for sequencing (Life Sciences kit) by TA cloning and sequenced by Sanger Sequencing at Penn State Genomics Facilities.

Cloning into pET14b Vector: The open reading frame of the LvSRT protein was cloned into XhoI/BamHI site of the pET-14b vector (Novagen). Digestions of the PCR products and the vector were carried out at 37 °C for 3 h, and purified using Qiagen PCR clean up. Purified PCR fragments were ligated using T4 ligase (New England Biolabs) with a ratio of 3:1 insert to vector. The gene was cloned omitting the predicted signaling peptide and in framed with the his-tag found in the pET-14b vector. The primers used to amplify the PCR product were: Forward primer 5′-TATA**CTCGAG**CTCCTTCCAGGTCTCTTGGGTG-3′; Reverse primer 5′-TATC**GGATCC**TTAGTAGAGACCGTATCCGAAACCTCCA-3′.

Expression of Recombinant SRT: A single colony was inoculated and grown overnight in 25 mL of LB with ampicillin (50 μg/mL). The overnight culture was inoculated into four 1-liter shake flask culture containing 500 mL of LB ampicillin (50 μg/mL). The culture was grown at 37 °C to an OD600 of 0.6 when IPTG was added to obtain an induction concentration of 0.5 mM for 4 h. The cells were then pelleted at 10 000 r.p.m. for 15 min and washed twice with 50 mL of 20 mM Tris buffer pH 8. The cell pellet was then resuspended in 50 mL of lysis buffer (50 mM Tris pH 7.4, 200 mM NaCl, 1 mM PMSF, 10 mg/ml lyzosyme, 0.1 mg/mL DNAse I, and 2 mM EDTA) and lysed using a high-pressure homogenizer. The lysed cells were pelleted at 14 000 r.p.m. for 1 h at 4 °C. The pellet was then washed twice with urea extraction buffer (100 mM Tris pH7.4, 5 mM EDTA, 2 M urea, 2% (v/v) Triton X-100, 5 mM DTT) and then twice with a wash buffer (100 mM Tris pH7.4, 5 mM EDTA, 5 mM DTT). The remaining pellet was then resolubilized in 5% acetic acid. Recombinant proteins of ≈90% purity were obtained in this manner and yields were estimated at ≈50 mg/L.

Expression of Recombinant SRT via Autoinduction Media: A single colony was inoculated in auto-induction media formulated by Studier[26] with ampicillin (50 μg/ml). The cultures were grown at 25 °C with agitation of 300 rpm until an OD above 8 was obtained. The cells were then pelleted at 10 000 r.p.m. for 15 min and washed twice with 50 mL of 20 mM Tris buffer pH 8. The cell pellet was then resuspended in 50 mL of lysis buffer (50 mM Tris pH 7.4, 200 mM NaCl, 1 mM PMSF, 10 mg/mL lyzosyme, 0.1 mg/mL DNAse I, and 2 mM EDTA) and lysed using a high-pressure homogenizer. The lysed cells were pelleted at 14 000 r.p.m. for 1 h at 4 °C. The pellet was then washed twice with urea extraction buffer (100 mM Tris pH7.4, 5 mM EDTA, 2 M urea, 2% (v/v) Triton X-100, 5 mM DTT) and then twice with a wash buffer (100 mM Tris pH7.4, 5 mM EDTA, 5 mM DTT). The remaining pellet was then resolubilized in 5% acetic acid and freeze dried using a Freezezone 12 (Labcono, Kansas City, MO). Recombinant proteins of ≈90% purity were obtained in this manner and yields were estimated at 0.19 gram protein per gram of dry biomass.

Thermo-Mechanical Characterization: Dynamic Mechanical Analysis (TA 800Q DMA) was performed in dry and wet conditions with film-tension and submersion-tension clamps, respectively. Sample dimensions were 15 mm × 2.5 mm × 0.2 mm for the dry test and 25 mm × 2 mm × 0.2 mm for the wet test. Stress–strain experiments were performed with a strain rate of 1% per minute and a preload of 0.01 N. Oscillatory temperature experiments were performed at 1 Hz, with amplitude of 2 μm and a rate of 2 °C per minute.

Supporting Information

Supporting Information is available from the Wiley Online Library or from the author.

Acknowledgements

A.P.-F. and S.F. contributed equally to this work. M.C.D. planned, developed and supervised the research. M.C.D. and A.P.-F. introduced the protein melt concept, characterized the surfaces, and performed the spectroscopic, mechanical and microscopy experiments. S.F. and H.J. worked on the RNA extraction and recombinant expression of the protein under the guidance of W.R.C. and M.C.D. A.S. and I.A. assembled the transcriptome and provided guidance in the area of bioinformatics. All authors contributed to writing and revising the manuscript, and agreed on its final contents. The authors thank Jeffrey Catchmark, Reginald Hamilton and Tugba Ozdemir at Penn State for their help with DMA, DSC, and electrospin experiments respectively. The authors gratefully acknowledge financial support for this work from the Office of Naval Research (N000141310595), Army Research Office (W911NF-14-P-0012) and technical support (Tatiana Laremore and Craig Praul) from the Genomics and Proteomic Facilities of the Huck Institute of Life Science at the Pennsylvania State University.

Received: June 13, 2014
Revised: July 28, 2014
Published online: September 11, 2014

[1] S. Kabasci, *Bio-Based Plastics: Materials and Applications*, John Wiley and Sons, UK **2013**.
[2] J. B. Van Beilen, Y. Poirier, *Plant J.* **2008**, *54*, 684.
[3] D. N. Rockwood, R. C. Preda, T. Yücel, X. Wang, M. L. Lovett, D. L. Kaplan, *Nat. Protoc.* **2011**, *6*, 1612.
[4] V. Hernandez-Izquierdo, J. Krochta, *J. Food Sci.* **2008**, *73*, R30.
[5] R. Langer, D. A. Tirrell, *Nature* **2004**, *428*, 487.
[6] R. L. DiMarco, S. C. Heilshorn, *Adv. Mater.* **2012**, *24*, 3923.
[7] X. Hu, P. Cebe, A. S. Weiss, F. Omenetto, D. L. Kaplan, *Mater. Today* **2012**, *15*, 208.
[8] B. J. Haas, A. Papanicolaou, M. Yassour, M. Grabherr, P. D. Blood, J. Bowden, M. B. Couger, D. Eccles, B. Li, M. Lieber, *Nat. Protoc.* **2013**, *8*, 1494.
[9] S. Pevtsov, I. Fedulova, H. Mirzaei, C. Buck, X. Zhang, *J. Proteome Res.* **2006**, *5*, 3018.
[10] P. A. Guerette, S. Hoon, Y. Seow, M. Raida, A. Masic, F. Tian, M. C. Demirel, A. Pena-Francesch, S. Amini, G. Tay, A. Miserez, *Nat. Biotechnol.* **2013**, *31*, 908.
[11] M. Nixon, P. Dilly, "Sucker surfaces and prey capture", presented at *Symp. Zool. Soc. Lond* **1977**.
[12] L. W. Williams, *The Anatomy of the Common Squid, Loligo Pealii: Lesueur*, Library and printing-office late EJ Brill, NY **1910**.
[13] A. Pena-Francesch, B. Akgun, A. Miserez, W. Zhu, H. Gao, M. C. Demirel, *Adv. Funct. Mater.* **2014**, DOI: 10.1002/adfm.201401534.
[14] A. Packard, *Biol. Rev.* **1972**, *47*, 241.
[15] A. W. Perriman, A. P. S. Brogan, H. Cölfen, N. Tsoureas, G. R. Owen, S. Mann, *Nat. Chem.* **2010**, *2*, 622.
[16] P. Privalov, N. Khechinashvili, *J. Mol. Biol.* **1974**, *86*, 665.
[17] M. C. Demirel, A. R. Atilgan, I. Bahar, R. L. Jernigan, B. Erman, *Protein Sci.* **1998**, *7*, 2522.
[18] K. Dorrington, N. McCrum, *Biopolymers* **1977**, *16*, 1201.
[19] A. Miserez, J. C. Weaver, P. B. Pedersen, T. Schneeberk, R. T. Hanlon, D. Kisailus, H. Birkedal, *Adv. Mater.* **2009**, *21*, 401.
[20] M. Steinhart, J. H. Wendorff, A. Greiner, R. B. Wehrspohn, K. Nielsch, J. Schilling, J. Choi, U. Gösele, *Science* **2002**, *296*, 1997.
[21] T. Takajima, K. Kajiwara, J. E. McIntyre, *Advanced Fiber Spinning Technology*, Taylor & Francis, UK **1994**.
[22] M. Yoshida, Y. Ishikura, T. Moritaki, E. Shoguchi, K. K. Shimizu, J. Sese, A. Ogura, *Gene* **2011**, *483*, 63.
[23] T. N. Petersen, S. Brunak, G. von Heijne, H. Nielsen, *Nat. Methods* **2011**, *8*, 785.
[24] P. J. Flory, *Principles of Polymer Chemistry: Paul J. Flory*, Cornell University **1953**.
[25] a) M. Nakanishi, R. Nozaki, *Phys. Rev. E* **2011**, *83*, 051503; b) R. Van der Sman, *Food Hydrocolloids* **2012**, *27*, 529.
[26] F. W. Studier, *Protein Expression Purification* **2005**, *41*, 207.
[27] M. J. Hancock, K. Sekeroglu, M. C. Demirel, *Adv. Funct. Mater.* **2012**, *22*, 2223.
[28] N. A. Malvadkar, M. J. Hancock, K. Sekeroglu, W. J. Dressick, M. C. Demirel, *Nat. Mater.* **2010**, *9*, 1023.
[29] E. So, M. C. Demirel, K. J. Wahl, *J. Phys. D: Appl. Phys.* **2010**, *43*, 045403.
[30] D. R. Maddison, K.-S. Schulz, Internet address: http://tolweb.org **2007**.